

# Lipoprotein lipase-mediated uptake of lipoprotein in human fibroblasts: evidence for an LDL receptor-independent internalization pathway

Mar Fernández-Borja,\* David Bellido,\* Elisabet Vilella,† Gunilla Olivecrona,§ and Senén Vilaró<sup>1,\*</sup>

Unit Cellular Biology,\* Department of Biochemistry and Physiology, University of Barcelona, E-08028 Barcelona, Spain; Centre de Recerca Biomèdica,† Hospital de Sant Joan, E-43201 Reus, Spain; and Department of Medical Biochemistry and Biophysics,§ University of Umea, S-901 87 Umea, Sweden

**Abstract** Lipoprotein lipase (LPL), a key enzyme in lipoprotein triglyceride metabolism, produces a marked increase in the retention and uptake of all classes of lipoproteins by cultured cells. It was previously shown that two different receptors are involved in mediating the LPL effects: heparan sulfate proteoglycans (HSPG) and the low density lipoprotein (LDL) receptor-related protein/ $\alpha_2$  macroglobulin receptor (LRP). By immunofluorescence we show here that cell surface-bound LPL displays a pattern that corresponds to the previously described distribution of cell surface HSPG. No evident relation to the distribution of bound activated  $\alpha_2$ -macroglobulin ( $\alpha_2$ M\*) or to LRP was observed. By immunoelectron microscopy we found that after 30 min at 37°C most of the detected  $\alpha_2$ M\* (70% of the total gold particles) was inside the cells and associated with endosomal vesicles. However, at the same time, 76% of the LPL remained at the cell surface, suggesting that LPL is internalized by a slow endocytic process. Binding of triglyceride-rich lipoproteins (TRL) or LDL together with LPL led to a spectacular increase in bound lipoproteins, which completely colocalized with LPL. After incubation at 37°C, LPL and 1,1'-dioctadecyl-3,3,3',3'-tetramethylindocarbocyanine (DiI)-TRL formed large clusters on the cell surface. Immunofluorescence and quantitative immunoelectron microscopy provided evidence of co-internalization of LPL and apoE-containing TRL by a slow endocytic process. In the absence of LPL, the fibroblasts rapidly internalized DiI-LDL and showed fluorescence in central, lysosome-like vesicles. In contrast, when LPL was present, internalization of DiI-LDL involved small, widely distributed vesicles. This pattern slowly changed to one consisting of large perinuclear vesicles. LDL receptor-deficient fibroblasts internalized DiI-LDL, either with or without LPL, into small widely distributed vesicles and no central vesicles were seen. Chloroquine-treated normal fibroblasts internalized DiI-LDL in a pattern similar to that of receptor-deficient fibroblasts. Taken together our results suggest an alternative receptor-independent endocytosis pathway for LDL. This pathway is potentiated by LPL and is characterized by a slow uptake involving small vesicles that gradually reach lysosomes. We suggest that, through its interaction with HSPG, LPL provides high capacity binding sites for lipoproteins and an independent internalization pathway.—**Fernández-Borja, M., D. Bellido, E. Vilella, G. Olivecrona, and S.**

**Vilaró.** Lipoprotein lipase-mediated uptake of lipoproteins in human fibroblasts: evidence for an LDL receptor-independent internalization pathway. *J. Lipid Res.* 1996. **37**: 464–481.

**Supplementary key words** heparan sulfate proteoglycans • triglyceride-rich lipoproteins • VLDL

The catabolism of chylomicrons and very low density lipoproteins (VLDL) is initiated by the hydrolysis of their triglycerides by the enzyme lipoprotein lipase (LPL) which is bound to the heparan sulfate proteoglycans (HSPG) on the luminal side of the vascular endothelium (1). Lipolysis by LPL causes a change in the lipid and protein composition of chylomicrons and VLDL, which become remnant particles and IDL-LDL, respectively (2). Remnant lipoproteins and LDL are eventually cleared from the circulation by specific apoE/apoB receptors in hepatic and extrahepatic tissues (3, 4). In turn, free fatty acids released by the lipase cause the detachment of LPL from the endothelium (5, 6). LPL circulates associated with cholesterol-rich lipoproteins (7, 8) and is cleared by the liver (9, 10). Recent studies (11, 12) have confirmed previous observations by Felts,

Abbreviations: ACAT, acyl-CoA:cholesterol acyltransferase; apo, apolipoprotein;  $\alpha_2$ M\*, activated  $\alpha_2$ -macroglobulin; bLPL, bovine lipoprotein lipase; BSA, bovine serum albumin; DiI, 1,1'-dioctadecyl-3,3,3',3'-tetramethylindocarbocyanine; FH, fibroblasts, LDL receptor-deficient fibroblasts; GPI, glycosyl phosphatidylinositol; IDL, intermediate density lipoproteins; LDL, low density lipoproteins; LRP, LDL receptor-related protein; HSPG, heparan sulfate proteoglycans; PBS, phosphate-buffered saline; RAP, receptor-associated protein; TRL, triglyceride-rich lipoproteins; VLDL, very low density lipoproteins.

<sup>1</sup>To whom correspondence should be addressed.

Itakura, and Crane (13), who proposed an additional role for LPL in the catabolism of lipoproteins by enhancing their binding and uptake by cells in a nonenzymatic mechanism.

LPL has high affinity for binding to HSPG (1) and several studies (14–22) indicate that these cell-surface molecules are involved in the LPL-mediated enhanced binding of lipoproteins to cultured cells. In addition to HSPG, other studies propose a novel receptor for LPL: the low density lipoprotein receptor-related protein- $\alpha_2$  macroglobulin receptor (hereafter referred to as LRP), which belongs to the LDL receptor family. LRP is a multifunctional receptor whose ligands include apoE,  $\alpha_2$ -macroglobulin, LPL, receptor-associated protein (RAP), tissue plasminogen activator, and lactoferrin (23). Because of its affinity for apoE-containing lipoproteins (24, 25), LRP has been postulated as the remnant receptor, although only lipoproteins artificially enriched in apoE are internalized by the LRP (26, 27). Recent experiments (28, 29) provide physiological evidence of the role of LRP in remnant clearance. On the other hand, LRP binds and mediates cellular catabolism of LPL (20, 30), which interacts with the receptor via its C-terminal domain (31, 32). In addition, it has been shown that LPL promotes binding of apoE-containing lipoproteins to LRP (11, 20).

The mechanism by which LPL potentiates the uptake and degradation of lipoproteins by cultured cells is not known in detail. To date three different possibilities have been proposed (33). One hypothesis holds that HSPG take part in the facilitated transfer of lipoproteins, bound via LPL, to specific lipoprotein receptors (LDL receptor and/or LRP) which are then responsible for endocytosis and final degradation (12, 13). Chappel et al. (19) showed that LPL induced uptake of normal triglyceride-rich lipoproteins by LRP. Mulder et al. (18) and Eisenberg et al. (16) concluded that LPL-enhanced uptake and degradation of LDL were mediated by the LDL receptor because LPL had no effect on LDL uptake by receptor-negative fibroblasts. Other authors (14, 15) propose that the LDL uptake and degradation mediated by LPL takes place via a receptor-independent, HSPG-mediated, slow internalization pathway. The third possibility is that both receptor-dependent and receptor-independent mechanisms are involved. This has been demonstrated for LPL-enhanced uptake of Lp[a] by fibroblasts (15).

In an attempt to elucidate the mechanisms involved in the LPL-enhanced binding and uptake of lipoproteins by cultured cells, we performed immunocytochemistry studies to examine the patterns of lipoprotein binding and internalization mediated by LPL. Using immunofluorescence and immunogold detection we studied binding and uptake of apoB- and apoE-containing

lipoproteins in the presence or absence of LPL by human normal and LDL receptor-deficient FH fibroblasts. The results provide direct morphological evidence for the proposed role of LPL as a bridge in the binding and internalization of lipoproteins and are consistent with a model in which part of the LPL-mediated increase in lipoprotein binding and uptake is mediated by a receptor-independent pathway, probably through HSPG.

## MATERIAL AND METHODS

### Materials

1,1',Dioctadecyl-3,3,3',3'-tetramethylindocarbocyanine (DiI) was purchased from Molecular Probes, Inc.; chloroquine, heparin, and bovine serum albumin (BSA, fraction V) were from Sigma. Two different antibodies to bovine lipoprotein lipase were used: a monoclonal antibody (2h10) obtained in the Barcelona laboratory (M. Fernández-Borja, E. Vilella, G. Olivecrona, and S. Vilaró, unpublished results) and an affinity-purified polyclonal antibody (poly66) raised in chicken (8). ApoE was detected by a rabbit polyclonal antibody kindly provided by Dr. U. Beisiegel (University of Hamburg, Germany). The monoclonal antibody to the  $\alpha$  subunit of LRP was a kind gift from Dr. J. Gliemann (Aarhus University, Denmark). Polyclonal antibody to human  $\alpha_2$ -macroglobulin was purchased from Dako. Fluorescein isothiocyanate (FITC)- and tetramethylrhodamine isothiocyanate (TRITC)-conjugated F(ab)<sub>2</sub> sheep anti-mouse IgG were from Boehringer Mannheim. TRITC-conjugated swine anti-rabbit immunoglobulins were from Dako. FITC-conjugated rabbit anti-chicken immunoglobulins were obtained from Sigma. Rabbit anti-chicken immunoglobulin was purchased from Nordic. Protein A-gold (10, 15, and 20 nm) were obtained from Dr. Slot (University of Utrecht, The Netherlands).  $\alpha_2$ -Macroglobulin ( $\alpha_2$ M) was purified from human plasma as described (34) and stored in 0.1 M sodium phosphate, pH 8.0, at -20°C.  $\alpha_2$ M was activated by incubation with 0.13 M methylamine for 1 h at room temperature. Bovine lipoprotein lipase (bLPL) was purified from milk as previously described (35). For biotinylation, LPL was dialyzed at 4°C for 8 h against 0.1 M Na-bicarbonate buffer, pH 8.8, containing 1 M NaCl. N-hydroxysuccinimide biotin was added (25  $\mu$ g/mg LPL) from a stock solution in dimethyl sulfoxide (10 mg/ml). After incubation at 4°C overnight, 1 M NH<sub>4</sub>Cl was added (20  $\mu$ l/250  $\mu$ g ester). After 15 min at 4°C the sample was diluted by addition of 2 volumes of 10 mM Bistris buffer, pH 6.5, and was immediately applied to a column of heparin-Sepharose that had been equilibrated in 10 mM Bistris, pH 6.5, containing 0.3 M NaCl.

After a brief wash, the column was eluted by a salt gradient (0.2 M NaCl–1.5 M NaCl). Biotinylated LPL appeared at the salt concentration expected for active LPL dimers. Activity measurements showed that the enzyme was fully active. For stabilization, 2 mg BSA/ml was added before storage at -70°C.

### Lipoprotein isolation and labeling

Blood was collected from normolipidemic and hyperlipidemic subjects and the plasma was separated by centrifugation at 500 g for 10 min. LDL (d 1.006–1.063 g/ml) from normolipidemic human plasma and triglyceride-rich lipoproteins (d <1.006 g/ml) from normolipidemic and hyperlipidemic human plasma were isolated by preparative ultracentrifugation (36). Lipoproteins were labeled with 1,1'-dioctadecyl-3,3,3',3'-tetramethylindocarbocyanine (DiI) by incubating the lipoproteins at 0.5 mg protein/ml in PBS–0.5% BSA with 100 µl of DiI in dimethyl sulfoxide (3 mg/ml) for 8 h at 37°C (25). The lipoproteins were overlaid with phosphate-buffered saline (PBS, 10 mM phosphate, 150 mM NaCl, pH 7.4) and reisolated by centrifugation (300,000 g, 16 h at 4°C). Lipoproteins were dialyzed against PBS and filtered before use. Protein content was determined by the BCA method (Pierce) using BSA as standard.

### Cell culture

Human skin fibroblasts were grown in Dulbecco's modified Eagle's medium (DMEM) with 10% fetal calf serum, penicillin, and streptomycin. Cells between the 4th and 15th passage were plated on glass coverslips (for fluorescence detection experiments) or 35-mm plastic culture dishes (for immunogold detection experiments) and used between the 3rd and 4th day after seeding. LDL receptor-deficient human skin fibroblasts (FH fibroblasts) were a kind gift from Dr. U. Beisiegel (Hamburg). FH fibroblasts were maintained under the same conditions as the normal fibroblasts.

### Cellular binding and internalization of lipoproteins

Fibroblasts used for LDL binding and uptake experiments were incubated with medium without serum for 16 h prior to the experiment. Cells on coverslips were prechilled to 4°C and washed with cold DMEM containing 20 mM HEPES, pH 7.4, and 1% BSA (DMEM-BSA) and binding experiments were performed by incubating the cells for 30 min at 4°C with DiI-labeled LDL (DiI-LDL) or DiI-labeled triglyceride-rich lipoproteins (DiI-TRL), at a concentration of 5 µg protein/ml, in the presence or absence of 2.5 µg bLPL/ml. After binding, medium was removed and fresh DMEM-BSA, previously warmed, was added to cells, which were then incubated at 37°C for different periods. After each period, cells

were washed in DMEM-BSA. Alternatively, and to examine cellular uptake of lipoproteins, cells were washed in DMEM-BSA containing 100 U heparin/ml for 15 min at 4°C with constant shaking. After washes, cells were fixed for 10 min at room temperature in 3% paraformaldehyde–2% sucrose in 0.1 M phosphate buffer, pH 7.4. Finally, coverslips were mounted up-side-down on a glass slide with a drop of Immunofluore mounting medium (ICN). Cells were observed and photographed using a Zeiss Axioskop.

### Chloroquine treatment

Cells on coverslips were pre-treated with 75 µM chloroquine in DMEM-BSA for 30 min at 37°C. Cells were then cooled to 4°C and incubated with DiI-LDL (5 µg protein/ml) for 30 min at 4°C. After binding, medium was replaced by fresh pre-warmed DMEM-BSA containing 75 µM chloroquine. After incubation for 1 h at 37°C, cells were washed in DMEM-BSA containing 100 U heparin/ml for 15 min at 4°C with constant shaking. Finally, cells were fixed and processed for observation as indicated above.

### Immunofluorescence detection

Immunodetection of cell surface-bound  $\alpha_2M^*$  after the incubation of the fibroblasts with 16 µg/ml of activated  $\alpha_2M$  for 1 h at 4°C was performed by using a polyclonal antibody to human  $\alpha_2M$  and an FITC-labeled secondary antibody. LRP was detected in fixed cells permeabilized with ice-cold acetone for 30 sec using a monoclonal antibody to the  $\alpha$  subunit and a TRITC-labeled secondary antibody. For double immunofluorescence of bound LPL and LRP, LPL was detected by using the polyclonal antibody poly66 and an FITC-rabbit anti-chicken IgG antibody.

Binding experiments on unlabeled TRL (10 µg protein/ml) in the presence/absence of LPL were performed as described above except that, after fixation, bound lipoproteins were detected by immunolabeling of apoE with specific polyclonal antibodies. Bound bLPL was also immunodetected using a monoclonal antibody (2h10) and by chicken anti-LPL. Briefly, cells were incubated for 45 min at 37°C with the primary antibody, washed in PBS, and incubated for a further 30 min with FITC- or TRITC-labeled secondary antibody. For double immunodetection, cells were incubated with a mixture of primary antibodies followed by an incubation with a mixture of non-crossreacting secondary antibodies.

### Electron microscopy studies

Binding and internalization of TRL by human fibroblasts in the presence or the absence of LPL was also studied by pre-embedding at the electron microscope.

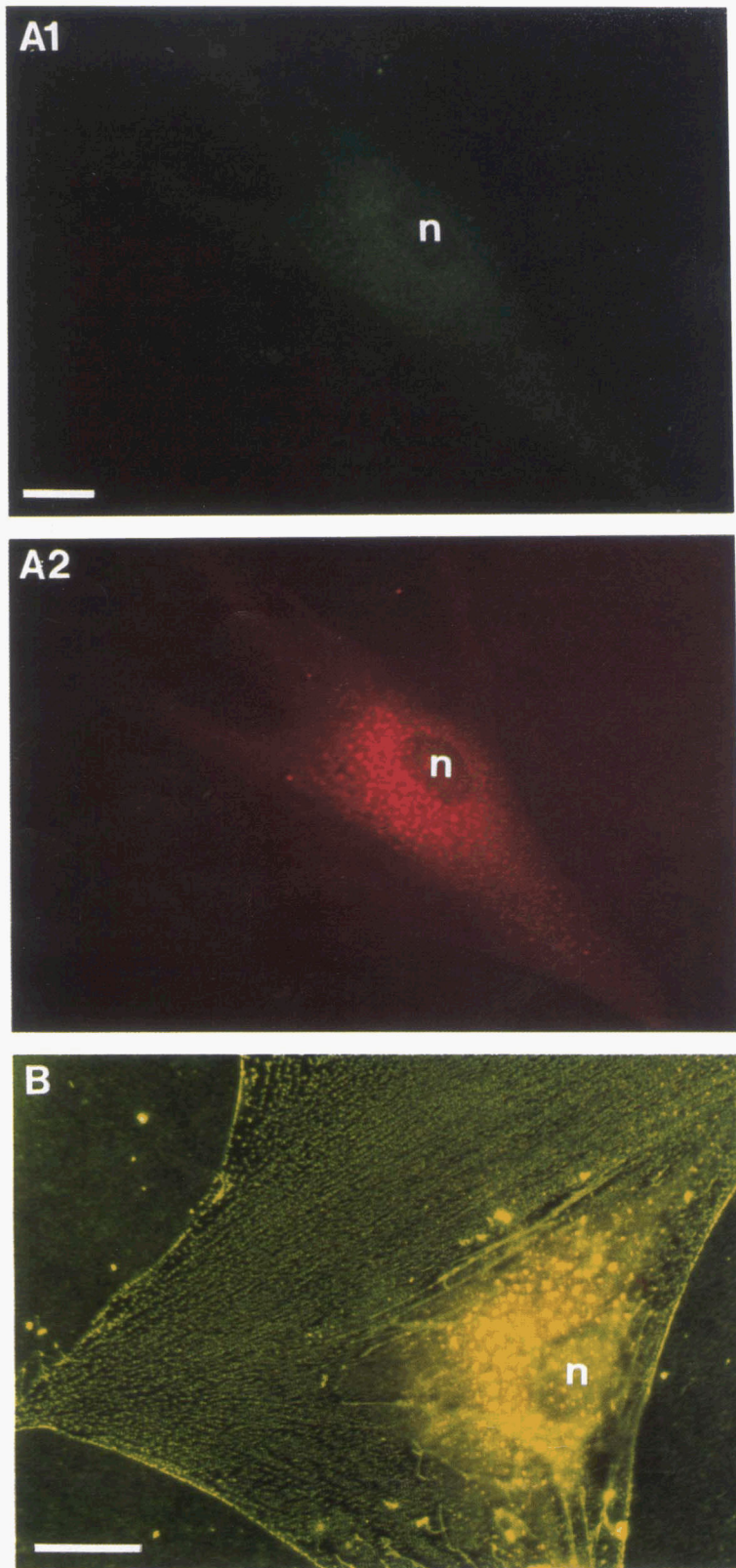


**Fig. 1.** Distribution of  $\alpha_2$ -macroglobulin and LPL on the fibroblast cell surface and the relation to LRP. Activated  $\alpha_2$ -macroglobulin (16  $\mu\text{g}/\text{ml}$ ) or bLPL (2.5  $\mu\text{g}/\text{ml}$ ) was bound to human skin fibroblasts at 4°C for 60 min. Cells were then fixed and permeabilized. Double immunofluorescence was performed to detect  $\alpha_2$ -macroglobulin and LRP (A1 and A2, respectively) or bLPL and LRP (B). B is a double exposure micrograph where LPL appears in green and LRP in orange. Note the difference in fluorescence intensity and the completely different binding patterns of

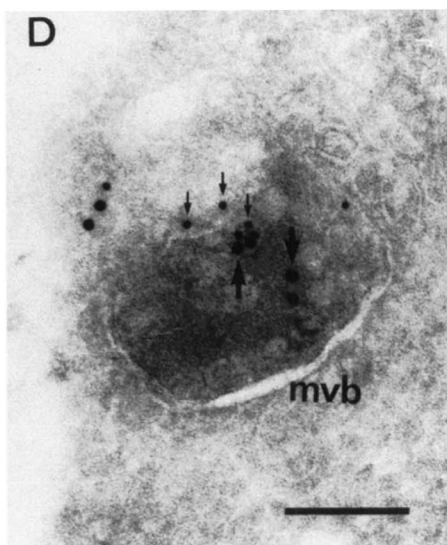
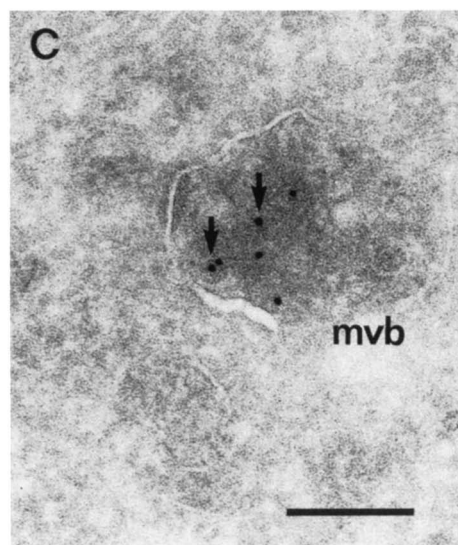
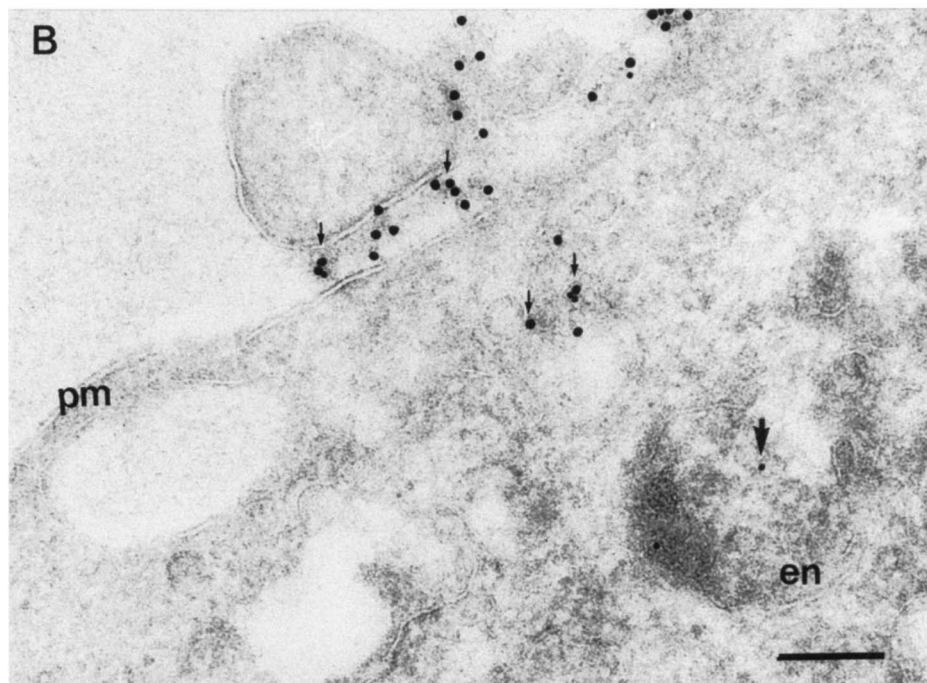
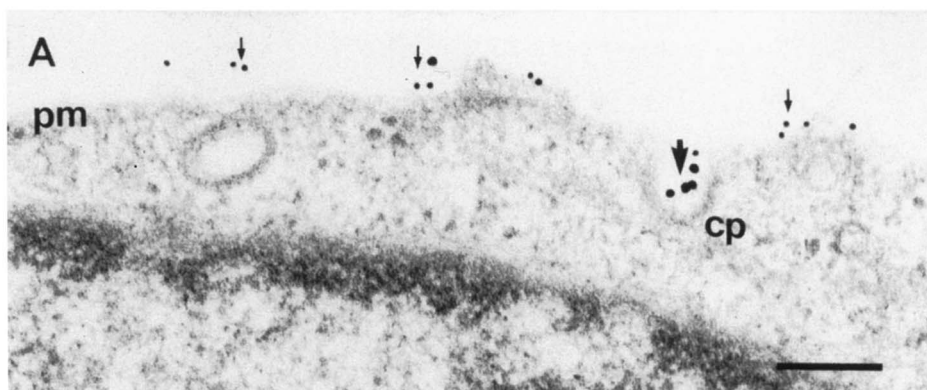


**Fig. 2.** Immunogold detection of bound and internalized  $\alpha_2$ -macroglobulin and LPL by fibroblasts. Equimolar concentrations of bLPL (2.5  $\mu\text{g}/\text{ml}$ ) and activated  $\alpha_2$ -macroglobulin (16  $\mu\text{g}/\text{ml}$ ) were bound together to cultured human fibroblasts for 1 h at 4°C. Bound proteins were visualized using pre-embedding techniques with goat anti-mouse-gold (10 nm, small arrows) for LPL and protein A-gold (15 nm, large arrows) for  $\alpha_2$ -macroglobulin (A). Internalization of both proteins after incubation of the cells for 30 min at 37°C was studied by cryoultramicrotomy procedures (B, C, D). Note that in this case LPL and  $\alpha_2$ -macroglobulin were detected with protein A-gold (15 nm) and (10 nm), respectively. Also note that LPL (labeled with the larger gold particles, small arrows) was still associated with the plasma membrane after 30 min at 37°C while all the  $\alpha_2\text{M}^*$  (small gold particles, large arrows) had been internalized. (pm, plasma membrane; cp, coated pit; en, endosome; mvb, multivesicular body). Bar 0.2  $\mu\text{m}$ .

Fibroblasts grown in 35 mm-diameter culture dishes were incubated for 1 h at 4°C with a mixture of TRL (10  $\mu\text{g}$  protein/ml) and 2.5  $\mu\text{g}/\text{ml}$  of biotin-conjugated bLPL. ApoE immunodetection was carried out by incubating the cells (30 min at 4°C) with a rabbit anti-human apoE antibody in buffer B, followed by a 30-min incubation at 4°C with protein A-gold (20 nm). LPL was immunodetected with streptavidin-gold (5 nm). Cells were then warmed to 37°C and incubated for 0, 30, 60, 180, and 480 min. After each time period cells were fixed in 2% paraformaldehyde–2.5% glutaraldehyde in phosphate buffer, scraped, and collected by centrifugation. Pellets were postfixated in 1%  $\text{OsO}_4$ , dehydrated, and embedded in Spurr for sectioning. Ultrathin sections (30–50 nm) were stained with uranyl acetate and lead citrate.

Immunodetection of cell surface-bound  $\alpha_2\text{M}^*$  was also carried out by the pre-embedding method. After the incubation of the fibroblasts with a mixture of 16  $\mu\text{g}/\text{ml}$  of  $\alpha_2\text{M}^*$  and 2.5  $\mu\text{g}/\text{ml}$  for 1 h at 4°C, cells were fixed for 1 h in 2% paraformaldehyde–0.1% glutaraldehyde in 0.1 M phosphate buffer, pH 7.4.  $\alpha_2\text{M}^*$  was immunodetected with rabbit antibody to human  $\alpha_2\text{M}^*$  and protein A-gold (15 nm), and LPL with monoclonal anti bovine-LPL and goat anti-mouse-gold (10 nm). After immunolabeling, cells were fixed in 2% paraformaldehyde, 2.5% glutaraldehyde, scraped, collected by centrifugation, and processed as indicated above. Internalization of  $\alpha_2\text{M}^*$  and LPL was followed by immunogold labeling of cryosections (post-embedding method). Binding was performed as indicated above with a mixture of  $\alpha_2\text{M}^*$  and LPL, and the cells were then warmed to 37°C and incubated for 30 min. Cells were fixed with 2% paraformaldehyde–0.2% glutaraldehyde in phosphate buffer, scraped, and collected by centrifugation. Cell pellets were embedded in 10% gelatin blocks and post-fixed overnight in 2% paraformaldehyde at 4°C. Blocks were cryoprotected in polyvinylpyrrolidone and 2% sucrose solution for 24 h, mounted on a metal stub, rapidly frozen in liquid nitrogen, and maintained at -196°C before microtomy. Ultrathin sections (60 nm–85 nm) were obtained by cryoultramicrotomy at -105°C, placed on gold grids (200 mesh) formvar-coated for transmission electron microscopy, and maintained in 100 mM PBS, pH 7.4, at 4°C. The grids were treated with

150 mM ammonium chloride in 10 mM PBS solution, rinsed in 10 mM PBS–glycine 20 mM solution, and then blocked in 0.5% ovalbumin in 10 mM PBS–glycine 20 mM solution at room temperature.  $\alpha_2\text{M}^*$  was immunodetected with rabbit antibody to human  $\alpha_2\text{M}^*$  and protein A-gold (10 nm), and LPL by the chicken anti-bovine LPL, rabbit anti-chicken and protein A-gold (15 nm) according to the method described by Slot et al. (37). After labeling, grids were contrasted in 0.03% uranyl acetate solution and a thin surface membrane of methylcellulose was applied. Control experiments were performed in parallel with every immunolocalization by omitting either the ligand or the primary antibody or both. Sections were observed by conventional TEM (Hitachi 600 AB).

The intra- and extracellular distribution of  $\alpha_2\text{M}^*$ , LPL and apoE was determined by counting the number of gold particles located either at the plasma membrane or inside intracellular vesicles (see Results). For each quantitated experiment, 10 blocks were cut from the pellet of cells from a single plate. Three blocks were randomly selected and cut to sections. Three grids among the many from each block were selected on the basis of good morphology at a magnification of 850; cells in these grids that showed a nuclear profile were randomly chosen and used for counting at 15,000 magnification. For each experiment, 20–24 profiles were scored. In pre-embedding experiments, labeling of nuclei and mitochondria was considered as nonspecific and therefore excluded from the counts. The data are expressed as a percentage of the total number of particles per cell profile to normalize the differences in labeling efficiency from plate to plate. Each value is the mean of three experiments and at least 500 particles counted in different sections.

## RESULTS

### Binding and internalization of LPL by fibroblasts

As the binding of LPL to LRP *in vitro* has been widely reported, our initial purpose was to visualize the distribution of the lipase on the fibroblast cell surface in relation to the distribution of LRP. Preliminary experiments (not shown) using monoclonal antibodies against

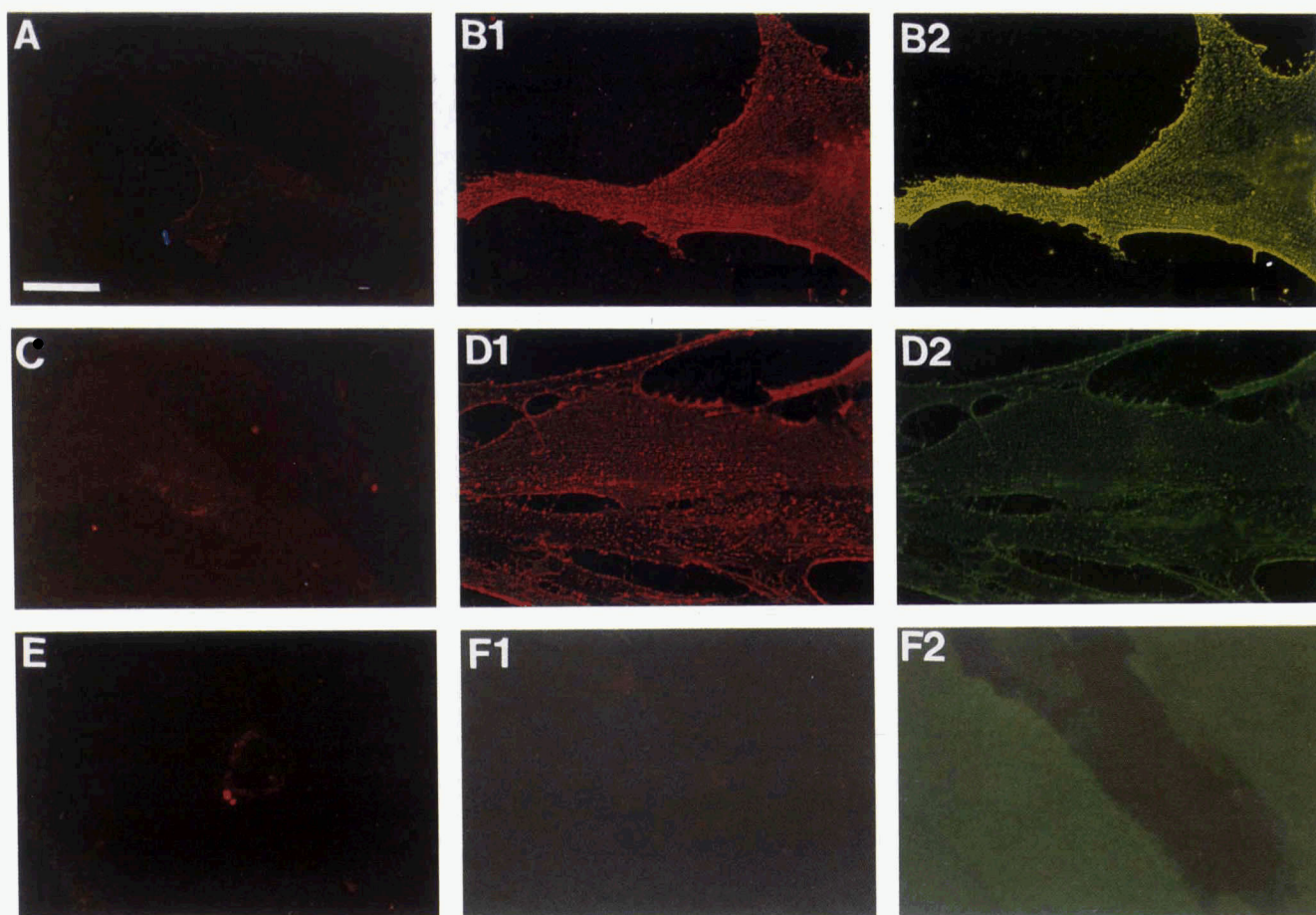


**Fig. 3.** LPL-mediated binding of TRL and LDL at the fibroblast cell surface. Human chylomicron remnants (TRL) (10  $\mu\text{g}$  protein/ml) were bound to cultured fibroblasts in the absence (A) or the presence (B) of bLPL. Bound TRL were detected by an anti-apoE and a TRITC-labeled secondary antibody (A and B1) and bound LPL was detected with a monoclonal antibody and a FITC-labeled secondary antibody (B2). DiI-labeled human LDL (5  $\mu\text{g}$  protein/ml) were bound in the absence (C) or the presence (D) of bLPL. LPL was immunodetected by a monoclonal antibody and an FITC-labeled secondary antibody (D2). Bound DiI-LDL without (E) or with (F) bLPL was displaced by 100 U/ml heparin. Bound bLPL was also displaced by the heparin (F2). Exposure times were identical for all the micrographs except for E, F1 and F2, which were overexposed. Bar 40  $\mu\text{m}$ .

$\alpha$  and  $\beta$  subunits of LRP showed very low immunofluorescence labeling on the non-permeabilized human fibroblast cell surface, suggesting that very little LRP is exposed at the cell surface. Then, we performed binding experiments at 4°C with  $\alpha_2$ -macroglobulin ( $\alpha_2\text{M}^*$ ), a specific ligand for LRP (38), to determine the cell surface distribution of this receptor molecule. The total (intracellular and plasma membrane-associated) LRP was detected by a monoclonal antibody to the  $\alpha$  subunit of the receptor. Cells were incubated at 4°C for 60 min with  $\alpha_2\text{M}^*$  (16  $\mu\text{g}/\text{ml}$ ), then permeabilized, and double immunofluorescence detection was performed with anti- $\alpha_2$ -macroglobulin and anti-LRP antibodies. **Figure 1A** shows the distribution of cell surface-bound  $\alpha_2\text{M}^*$  and of both cell-surface and intracellular LRP. As detected by immunofluorescence, very little  $\alpha_2\text{M}^*$  bound to the cell surface, and only to the central zone of the cell (Fig. 1 A1), indicating that plasma membrane-asso-

ciated LRP is very low and restricted to the central area of the cell. Immunofluorescence detection of total LRP (Fig. 1 A2) (intracellular and plasma membrane) indicated that most of the receptor is found within the cell in perinuclear vesicles. When dimeric, active bovine LPL (2.5  $\mu\text{g}/\text{ml}$ ) was used for binding experiments, a strikingly different cell surface immunofluorescence pattern was observed (Fig. 1B). LPL bound to fibroblasts on their whole surface in a very characteristic pattern. The cells presented a fine punctate staining consisting of small fluorescent clusters organized in parallel linear arrays that crossed the fibroblast cell surface longitudinally (Fig. 1B). Intense fluorescent labeling was observed at the edges of the cells. We have previously shown that this characteristic pattern corresponds to the fibroblast cell surface distribution of HSPG, which are organized by the actin cytoskeleton (39). When LRP was also immunodetected in the same cells, no evident

relation was found between LRP and LPL (Fig. 1B), indicating that very little of the initial binding of LPL at the fibroblast cell surface could be explained by binding to plasma membrane LRP.

The binding of LPL and  $\alpha_2M^*$  was also examined by electron microscopy. Colloidal gold particles were used to detect the ligands using either the pre-embedding or the post-embedding technique (Fig. 2). After binding of LPL (2.5  $\mu\text{g}/\text{ml}$ ) together with  $\alpha_2M^*$  (16  $\mu\text{g}/\text{ml}$ ) the distribution of these proteins on the cell surface differed. While labeling for  $\alpha_2M^*$  was mainly associated with coated pits (87.5% of the total gold particles) (Fig. 2A, large arrows), labeling of LPL appeared in clusters and was not restricted to specific domains of the cell surface (only 5.7% of the total gold particles were associated to coated pits) (Fig. 2A, small arrows). Cells were incubated for 30 min at 37°C with LPL and  $\alpha_2M^*$  and internalization of both proteins was followed by cryoultramicrotomy and immunocytochemistry. Figure 2 (B to D), shows cellular structures where LPL and  $\alpha_2M^*$  were found. After 30 min at 37°C, most of the immunodetected  $\alpha_2M^*$  was intracellular and associated with endosomal vesicles (70% of the gold particles) (Fig. 2 B–D; large arrows). However, immunogold detection of LPL indicated that 76% of this protein remained on the cell surface after 30 min incubation (Fig. 2B; small arrows). Nevertheless, a small amount of LPL (24%) was found intracellularly associated with endosomal structures (Fig. 2B and D, small arrows). Occasionally LPL and  $\alpha_2M^*$  were found together in membranous structures that resembled multivesicular bodies (Fig. 2D). Thus, little of the surface-bound LPL had been internalized after 30 min incubation, and not all of the internalized LPL was colocalized with  $\alpha_2M^*$ , suggesting that cell surface receptors other than LRP could be involved in LPL uptake.

#### LPL mediates binding of TRL and of LDL to cell surface HSPG

It is now very well documented that LPL mediates both binding and uptake of radiolabeled lipoproteins by several types of cells including fibroblasts (11, 12, 14–22). As the experiments reported above indicated that the initial binding of LPL was predominantly to the HSPG, we attempted to determine whether the cell surface distribution of lipoproteins and LPL after binding was the same and whether lipoproteins were internalized in the same endocytic structures. In order to determine the distribution pattern of lipoproteins on the surface of cultured fibroblasts, we performed binding experiments with lipoproteins in the absence or presence of LPL. Bound lipoproteins were detected either directly (DiI-labeled) or after immunolabeling with anti-apoE or anti-apoB antibodies and TRITC-con-

jugated goat anti-rabbit IgG. Figure 3 shows the binding of TRL, detected by apoE immunolabeling, and that of DiI-LDL in the absence (A, C) or the presence (B, D) of LPL. Binding of lipoproteins without LPL was not detectable by fluorescence for any of the ligands. However, in the presence of LPL, a prominent binding of lipoproteins to the whole cell surface was observed. Bound lipoproteins colocalized with LPL, and displayed the same characteristic binding pattern, organized in parallel arrays, as that found when cells are incubated with LPL alone (Fig. 1). As indicated above, this binding pattern reflects the cell surface distribution of HSPG. Identical patterns were observed when DiI-TRL or unlabeled LDL were used (results not shown). DiI-labeled LDL and nonlabeled TRL showed the same pattern, indicating that labeling with DiI did not influence the behavior of the lipoprotein particle. Heparin (100 U/ml) efficiently displaced bound lipoproteins and LPL (Fig. 3E and F), indicating that binding sites are sensitive to heparin.

#### LPL mediates cell internalization of TRL

Cell association of DiI-TRL at 37°C was higher when the lipase was present (Fig. 4, right column) than in its absence (Fig. 4, left column). After 15 min incubation in the absence of LPL, most of the DiI-TRL appeared internalized in large central vesicles. In contrast, cells incubated with DiI-TRL plus LPL showed a fluorescence pattern consisting of clusters on the cell surface. Double immunolabeling for apoE and for LPL indicated that this clustering occurred for both TRL and LPL (Fig. 5). At longer incubation times, cells incubated with DiI-TRL alone progressively accumulated fluorescence in central perinuclear vesicles, probably corresponding to lysosomes (Fig. 4). In the presence of LPL, cells also showed progressive accumulation of fluorescence in central vesicles, but even after 2 h incubation the fluorescence appeared widely distributed.

To test whether TRL were internalized together with LPL by human fibroblasts we used immunoelectron microscopy (Fig. 6). Pre-embedding immunocytochemistry with antibodies to LPL and to apoE revealed that, after binding at 4°C, LPL and TRL were in close association (Fig. 6A and B). Gold-label for LPL was detected surrounding the base of TRL (Fig. 6B), suggesting that LPL bridge lipid particles to the HSPG. After 30 min incubation at 37°C, large clusters of LPL and apoE labeling TRL were observed on the fibroblast cell surface (Fig. 6C). By this time, intracellular vesicles, probably endosomes, giving positive immunoreaction both for LPL and for apoE were also present (Fig. 6D). At longer incubation times (180 min), the label was detected inside electron-dense structures that could correspond to lysosomes (Fig. 6F). The cellular distribution



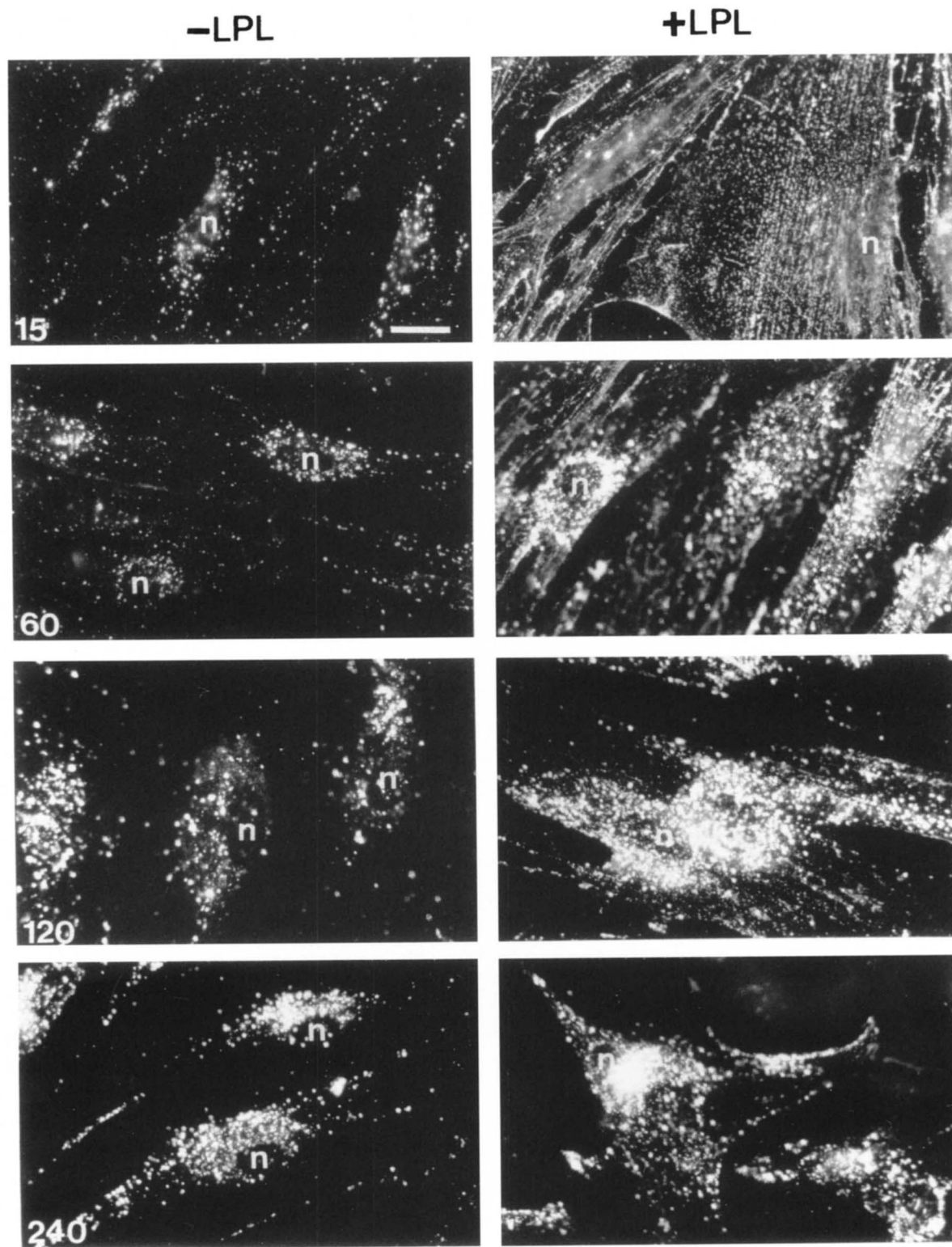


**Fig. 4.** Uptake of DiI-TRL in the presence or absence of LPL. Human fibroblasts were incubated with DiI-labeled TRL (5  $\mu\text{g}$  protein/ml) with (+LPL) or without (-LPL) bLPL (2.5  $\mu\text{g}/\text{ml}$ ) for 30 min at 4°C, washed, and then incubated for 15, 60, 120, and 240 min at 37°C. Cells were fixed and finally photographed. Exposure times were identical for all the micrographs. (n, nucleus). Bar 25  $\mu\text{m}$ .

of LPL and apoE at different incubation times was also determined by counting the number of gold particles in the plasma membrane or inside intracellular vesicles

(**Fig. 7**). After 15 min at 37°C, a small percentage of the gold particles (19% of the LPL and 18% of the apoE) was detected inside the cells. At 30 min the percentage

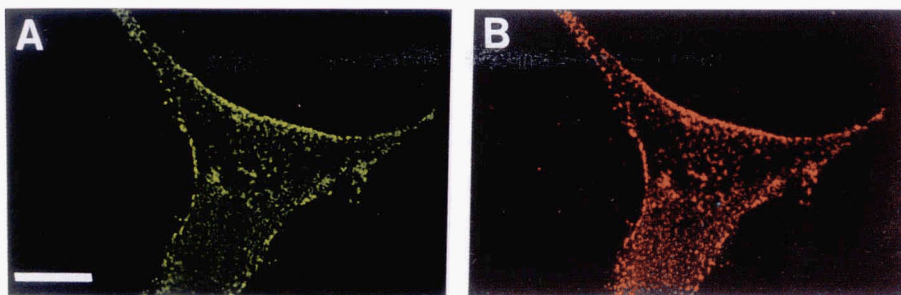


**Fig. 5.** Cell surface clustering of TRL in presence of LPL. After binding of TRL and bLPL to fibroblasts, the cells were incubated for 30 min at 37°C and then fixed. Cell surface LPL (A) was detected with a monoclonal anti-LPL and FITC-labeled goat anti-mouse and TRL (B) were detected polyclonal anti-apoE and TRITC-labeled secondary antibodies, as indicated in Material and Methods. Bar 40  $\mu$ m.

of intracellular labeling for both LPL and ApoE increased slightly, but most of the label was still in the plasma membrane, in strong contrast to what was observed for  $\alpha_2M^*$  (see above). At longer incubation times (180 and 480 min) the percentage of intracellular label (approximately 60%) increased, but still a substantial number of gold particles was detected at the plasma membrane. From these experiments it was noted that the changes observed in the gold particle distribution of both LPL and apoE were always equivalent. Thus, these results suggest that LPL and TRL are internalized together after clustering at the fibroblast cell surface, by a slow internalization process.

#### Receptor-independent pathway is involved in the LPL-mediated internalization of LDL

Next we attempted to determine whether the presence of LPL could influence the uptake of DiI-LDL by starved normal fibroblasts. After binding of DiI-LDL with or without LPL at 4°C, cells were incubated for different periods at 37°C. Then the cells were washed in DMEM-BSA containing 100 U heparin/ml to remove lipoproteins associated with cell membranes (as shown in Fig. 3, heparin completely displaces bound lipoproteins). The internalization pattern of DiI-LDL was strikingly different depending on whether LPL was present or not. In the absence of LPL, the DiI-LDL internalization pattern (Fig. 8, left column) consisted of large central vesicles that evolved into strongly labeled perinuclear vesicles corresponding to lysosomes. The progressive increase in fluorescence labeling observed at longer incubation may have been a consequence of the DiI-LDL accumulation inside the cell. In the presence of LPL, the pattern of internalized DiI-LDL (Fig. 8, right column) was completely different, especially after short incubation times (15 and 30 min). In this case, DiI-LDL was found in small vesicles extending out to the edges of the cell. After 15 min, little of the cell-associated DiI-LDL had been internalized. By 30 min, DiI-LDL fluorescence

was found in very small vesicles widely distributed throughout the cytoplasm as well as at the cell edges, which appeared heavily labeled. By 1 h some fluorescence started to concentrate in the cell center in large, bright vesicles, although small widely distributed vesicles were still present. In contrast, after the same incubation time, the fluorescence pattern displayed by cells incubated with DiI-LDL alone appeared almost exclusively as bright perinuclear vesicles. Only after 4 h incubation was a resemblance observed between the DiI-LDL patterns, which consisted of large central vesicles (lysosomes), in both the absence and in the presence of LPL. Furthermore, the fluorescence at the cell edges progressively disappeared, suggesting a slow edge-to-center intracellular routing for internalized LDL when associated with LPL. Parallel immunoelectron experiments showed that like TRL (see above), LDL were internalized together with LPL (not shown).

Internalization of DiI-LDL in the presence/absence of LPL was studied in LDL receptor-negative FH fibroblasts in order to discriminate between LDL receptor-dependent and receptor-independent internalization pathways. Similar to what was found with normal fibroblasts, binding of DiI-LDL was virtually undetectable when LPL was not present. With LPL, DiI-LDL gave a punctate pattern extending over the whole surface (results not shown). The internalization patterns were completely different in normal and FH fibroblasts (Fig. 9). After 1 h incubation at 37°C of normal fibroblasts with DiI-LDL, fluorescence appeared in large perinuclear vesicles. In contrast, FH fibroblasts were devoid of central vesicles and the pattern consisted of small vesicles distributed throughout the cytoplasm (Fig. 9). In the presence of LPL, normal fibroblasts showed both small widely distributed and large central vesicles. Note that in this case the central vesicles are not perinuclear and not lysosome-like, suggesting that LDL associated with LPL are internalized by a somewhat slower pathway compared to LDL alone. In FH fibroblasts, the fluores-

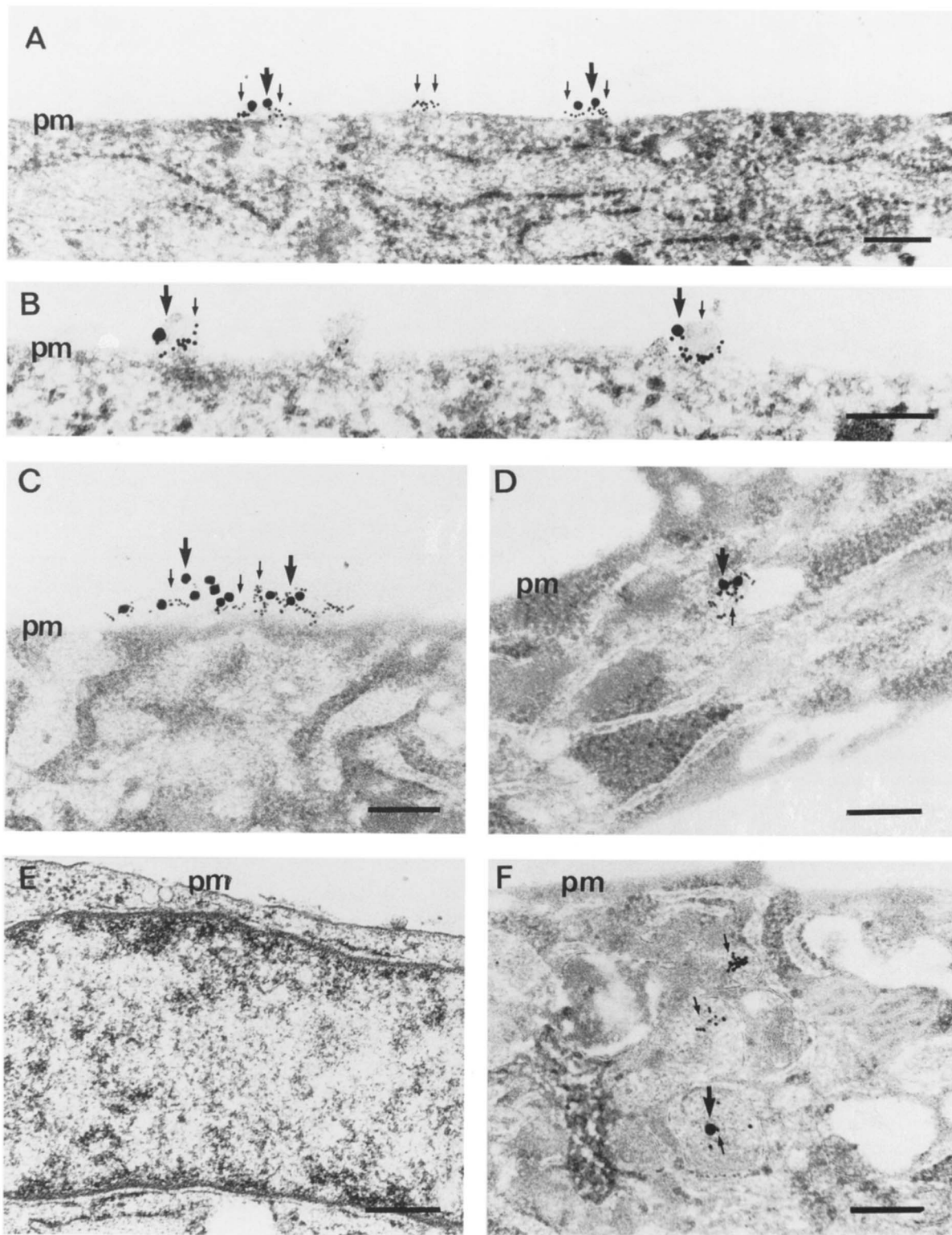


**Fig. 6.** Electron microscopy detection of bound and internalized LPL-TRL complexes. TRL and bLPL were bound to human fibroblasts and the cells were processed by pre-embedding techniques for the immunogold detection of apoE with protein A-gold (20 nm) and of biotin-LPL with streptavidin-gold (5 nm) (A, B). Internalization of the bound ligands was studied after incubation of the cells at 37°C for 30 min (C, D) and 180 min (F). Control experiments were performed in which incubation with TRL and LPL were omitted (E). Note the clustering of TRL and LPL at the plasma membrane during the 30 min incubation (C). (big arrows, TRL; small arrows, LPL; pm, plasma membrane). Bar 0.2  $\mu$ m.

cence pattern of DiI-LDL plus LPL was essentially similar to the DiI-LDL pattern but with more heavily labeled vesicles (Fig. 9).

The results described above suggested that LDL uptake takes place both via a receptor-dependent and also via a receptor-independent pathway that is enhanced by LPL. To characterize the two pathways, we studied their respective sensitivity to chloroquine. By increasing the pH of intracellular vesicles, chloroquine inhibits cellular degradation of endocytosed ligands that accumulate in endosomes in association with their receptors (40). Chloroquine-treated normal fibroblasts incubated with either DiI-LDL or DiI-LDL plus LPL (Fig. 9) showed a fluorescence pattern devoid of central vesicles while the pattern of small vesicles remained. As could be expected, chloroquine-treated FH fibroblasts incubated either with DiI-LDL or DiI-LDL plus LPL (Fig. 9) displayed basically identical patterns to nontreated cells. These results indicate that after 1 h internalization, the receptor-dependent pathway is more sensitive to chloroquine than the receptor-independent pathway.

## DISCUSSION

These experiments were designed to explore the cellular interactions between LPL and lipoproteins. The current results provide immunocytochemical evidence that human fibroblasts present a high binding capacity for LPL which is probably associated with cell surface HSPG. We also show that LPL binds simultaneously to HSPG and to lipoproteins mediating the binding and internalization of TRL and LDL by human fibroblasts. Furthermore, our results suggest that the LPL-mediated uptake of lipoproteins mainly involves a receptor-independent pathway.

LPL binding sites cover the whole fibroblast cell surface, displaying a pattern organized in parallel arrays. In a recent study (39) we have shown that this pattern

corresponds to the cell surface organization of HSPG, which is mediated by the actin cytoskeleton (39, 41). In addition to HSPG, LPL binds to LRP (11, 19, 20, 30–32), which has been shown mediate the endocytosis and degradation of LPL by several cell types. Our double immunofluorescence and immunoelectron microscopy results seem to indicate that LRP has minor role, if any, in the initial binding of LPL at the cell surface of fibroblasts. As judged from binding of  $\alpha_2$ -macroglobulin at 4°C, only few LRP molecules are present on the human fibroblast cell surface. This is not surprising as most of the LRP is detected in intracellular vesicles by immunofluorescence and extracellular LRP is associated with coated pits on the cell surface (23) and these structures comprise only 2% of the surface of human fibroblasts (42). We observed that after incubation of the cells at 37°C with LPL together with  $\alpha_2$ M\*, some LPL molecules were found inside  $\alpha_2$ M\*-containing endocytic vesicles, suggesting that LRP could internalize part of the cell surface-bound LPL. Nevertheless, other LRP-independent pathways for LPL internalization must operate. This is suggested by the observation that some endocytosed LPL molecules did not colocalize with  $\alpha_2$ M\* and that, after incubation at 37°C for 30 min and longer (not shown), a large fraction of the LPL remained bound to the fibroblast cell surface. At this time all the  $\alpha_2$ M\* was found intracellularly. The hypothesis of a receptor-independent endocytosis is supported by two kinds of evidence. Previous results showed that the receptor-associated protein (RAP), which inhibits the binding of all known ligands to LRP, caused only a 43% decrease in the cellular degradation of LPL (21). Recently, Sehayek et al. (22) showed that degradation of  $^{125}$ I-labeled LPL was reduced by 60–70% in both HepG2 cells and in normal fibroblasts after the cells had been treated with sodium chlorate and heparinase to reduce their content of HSPG. In addition heparan sulfate-deficient CHO cells showed a low capacity to bind and degrade LPL (only 10% that of the wild

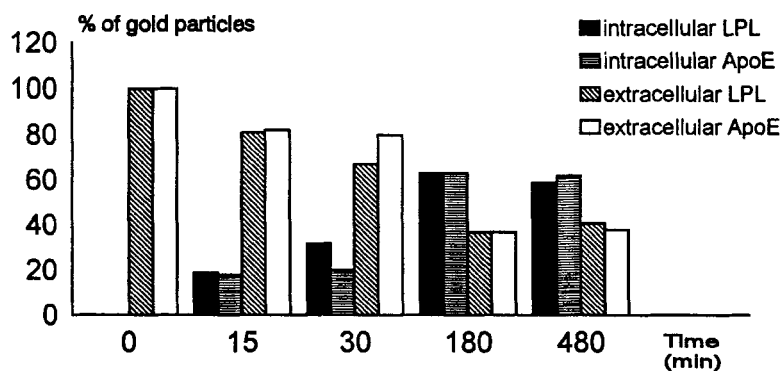
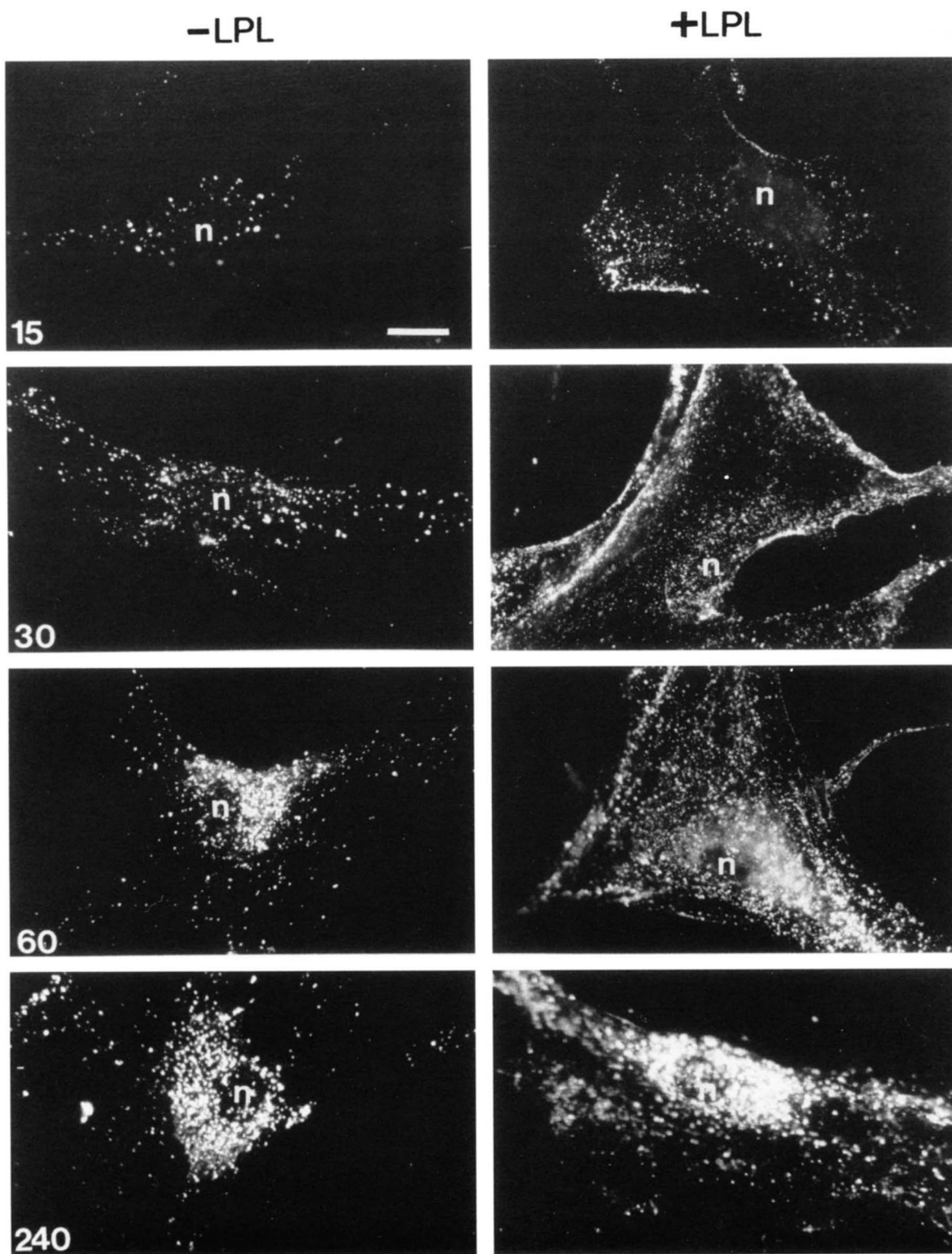


Fig. 7. Relative quantification of cellular distribution of LPL and apoE gold labeling. Human fibroblasts were incubated with TRL (5  $\mu$ g protein/ml) and bLPL (2.5  $\mu$ g/ml) for 30 min at 4°C, washed, and then incubated for the indicated times at 37°C and processed for electron microscopy as in Fig. 6. Gold particles located at the plasma membrane were counted and assigned as non-internalized LPL or ApoE. Gold particles located inside intracellular vesicles were assigned as internalized LPL or ApoE. Values are expressed as percentage of the total number of gold particles and represent the mean of three separate experiments. Variation between the mean values was less than 20%.



**Fig. 8.** Uptake of DiI-LDL in presence or absence of LPL. Human fibroblasts were incubated with DiI-labeled LDL (5  $\mu\text{g}$  protein/ml) in the absence (-LPL) or the presence (+LPL) bLPL (2.5  $\mu\text{g}/\text{ml}$ ) for 30 min at 4°C. They were washed and warmed to 37°C for 15, 30, 60, and 240 min. Cells were washed with 100 U/ml heparin to remove cell surface-bound lipoproteins and fixed. Exposure times were identical for all the micrographs. (n, nucleus). Bar 25  $\mu\text{m}$ .

type cells). These results taken together indicate that HSPG has an important role in the LPL metabolism. Like other coated pit-associated receptors, LRP undergoes rapid internalization upon ligand binding (43). Previous results obtained by Yanagishita (44) on HSPG metabolism by rat granulosa ovarian cells in culture show that membrane-intercalated and glycosyl phosphatidylinositol (GPI)-anchored HSPG are slowly internalized with a half-time of 4 h and 3 h, respectively. This could explain the long retention time of LPL bound to HSPG on the membrane.

The results presented here, showing that the presence of LPL causes a spectacular increase in the amount of lipoproteins bound to fibroblasts at 4°C, corroborate those reported by others using radiolabeled lipoproteins (11, 12, 14–22). By using immunofluorescence we observed that lipoproteins and LPL display identical binding patterns, suggesting that the lipase bridges the lipoproteins and the cell surface HSPG. By immunoelectron microscopy, we detected a close association of LPL with lipoproteins at the fibroblast cell surface. Our data are the first direct evidence of the putative role of LPL in mediating lipoprotein binding to HSPG on the membrane of cultured cells (12, 14–22). The interaction between lipoproteins and LPL may take place by means of the lipid moiety of the lipoproteins, as we obtained identical results with TRL and LDL, which have different apolipoprotein compositions. In fact, LPL promotes cellular binding of all classes of lipoproteins (16) and of apolipoprotein-free triglyceride emulsions (14). However, an interaction between LPL and certain apolipoproteins cannot be ruled out. Recently Sivaram et al. (45) showed that LPL specifically associates with the NH<sub>2</sub>-terminal region of apoB. We observed that LPL enhances the cellular association of lipoproteins more than cellular uptake, as examined after the removal of membrane-associated lipoproteins with heparin. Lipoprotein-LPL complexes form clusters on the cell surface that are subsequently internalized, as shown by immunogold microscopy. In an earlier study (39) we showed that these clusters are formed by an LPL-induced movement of HSPG along actin filaments.

From our results it is clear that, after internalization, lipoproteins follow different intracellular routing depending on the presence or absence of LPL, irrespective of their apolipoprotein composition. The internalization patterns were markedly different: endocytosed LDL was found in bright central vesicles (lysosomes), which became more fluorescent over the incubation time; in contrast, the pattern of LDL internalized in the presence of LPL consisted of small vesicles throughout the cytoplasm, especially extending out of the edge of the cell. After only 1 h of incubation, large central vesicles began to appear, although a diffuse pattern of

small vesicles could be still observed. After 4 h the two patterns became similar, indicating that, although more slowly, LDL internalized via LPL are also routed to lysosomes. The results obtained with FH fibroblasts further supported an internalization pathway mediated by HSPG. As previously described by Goldstein and Brown (46) LDL-receptor defective fibroblasts internalize and degrade LDL through a nonsaturable receptor-independent pathway. Attie et al. (47) also showed a receptor-independent pathway for LDL uptake by hepatocytes from rabbits lacking LDL receptors (Watanabe heritable hyperlipidemic rabbits). It has been shown (48, 49) that LDL bind to proteoglycans of the arterial wall, although with low affinity. In the present study, we show that FH fibroblasts internalize LDL according to a pattern which resembles that of LPL-mediated uptake by normal fibroblasts: diffuse small vesicles throughout the cytoplasm. Consistently, this pattern was identical either in the presence or absence of LPL, although more fluorescence was internalized in the presence of the lipase. It is not probable that LRP is involved in the binding and internalization of LDL by FH fibroblasts, as the enzyme was unable to mediate binding of LDL to LRP in ligand blotting experiments (20). Unlike normal fibroblasts, FH fibroblasts did not display central vesicles after 1 h incubation but did so after 4 h incubation.

These results confirm previous observations (14, 15, 18) of two distinct internalization pathways for LDL: a fast receptor-dependent pathway mediated by the LDL-receptor and a slow receptor-independent pathway mediated by HSPG and potentiated by LPL. These pathways differ in their intracellular routing: a special feature of the receptor-dependent pathway is the rapid central internalization of LDL, while the HSPG-mediated pathway is characterized by slow internalization into widely distributed vesicles. Interestingly, these pathways were affected differently by chloroquine treatment. Chloroquine-treated normal fibroblasts are devoid of fluorescent central vesicles after 1 h incubation with DiI-LDL, either in the presence or the absence of LPL. However, in the presence of LPL, the pattern of widely distributed vesicles persisted. Consistent with these observations, the LDL internalization pattern shown by FH fibroblasts was not affected by chloroquine in any case. The mechanism of chloroquine is based on the increase in intravesicular pH, which causes accumulation in the primary endosomes of internalized LDL, which cannot separate from the receptors (40). This leads to inhibition of the degradation of LDL (50) and prevents the LDL-receptor recycling to the cell membrane. In our understanding this may explain why no fluorescence was detected in chloroquine-treated normal fibroblasts after 1 h incubation with LDL. If the LDL-receptor cannot recycle, the total amount of LDL that could be internalized would be lower.

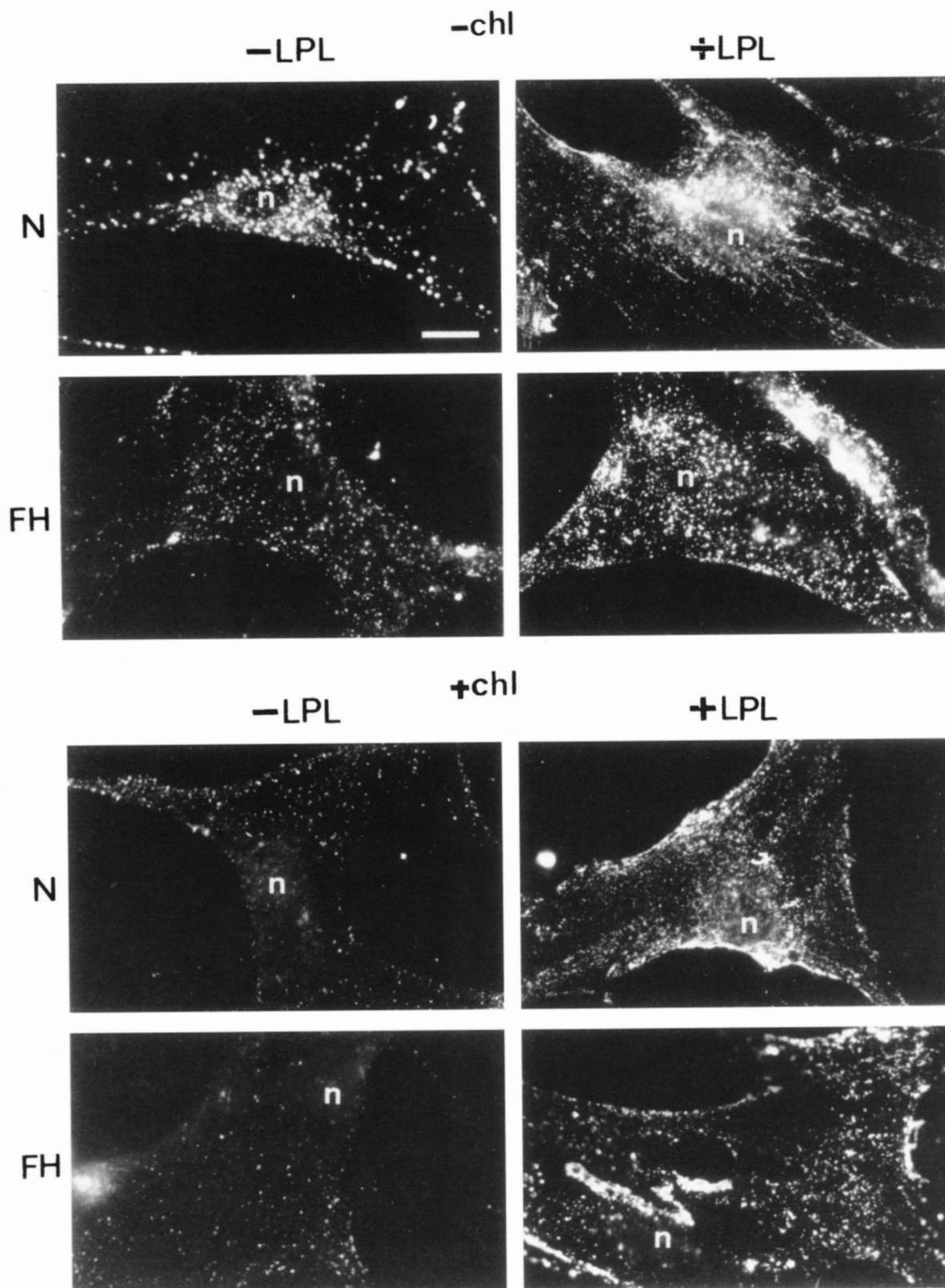


**Fig. 9.** Internalization of DiI-LDL by FH fibroblasts. Effect of chloroquine. Normal (N) and receptor deficient (FH) fibroblasts were either nontreated (-Chl) or treated (+Chl) with chloroquine and then incubated with DiI-LDL in the absence (-LPL) or the presence (+LPL) of bLPL for 30 min at 4°C. Cells were then washed and warmed to 37°C for 1 h to allow internalization. Cell surface lipoproteins were removed by heparin wash and the cells were fixed. Exposure times were identical for all the micrographs. (n, nucleus). Bar 25  $\mu$ m.

The operation of two internalization pathways, a specific receptor-mediated and an HSPG-mediated, has been described for another heparin-binding molecule, the basic fibroblast growth factor (bFGF) (51–53). In addition, Reiland and Rapraeger (53) showed that bFGF was targeted to different intracellular sites by the two receptors. Furthermore, in relation to lipoprotein metabolism, Tabas et al. (54) found different intracellular routing for internalized  $\beta$ -VLDL and LDL in macrophages. These authors postulated that the greater stimulation of ACAT by  $\beta$ -VLDL was due to the targeting of the two lipoproteins to different organelles with different ability to interact with microsomal ACAT. Lombardi et al. (55) suggested that different intracellular transport of VLDL and LDL in HepG2 cells was the cause of their differential effects on ACAT stimulation. One can speculate that the different routing provided by LPL-HSPG and the fact that HSPG are not subjected to down-regulation by the cellular sterol content may be the keys to understanding the possible physiological role of the LPL-mediated binding and uptake of lipoproteins. The sites where these events may be especially important would be those with a high concentration of LPL, such as the space of Disse (56), the endothelial surfaces (57), and the arterial wall (58). In this last location, LPL may be related to atherogenesis as it has been shown that LPL increases the retention of LDL by the subendothelial matrix (59, 60).

Finally, although our results cannot rule out the hypothesis proposed by several authors (18–20) that HSPG facilitate the transfer of lipoproteins bound via the lipase to the specific receptors for internalization, they do demonstrate that this is not the only internalization pathway. In conclusion, LPL provides high capacity binding sites for lipoproteins on the fibroblast cell membrane and an LDL receptor/LRP-independent internalization pathway which is not regulated by the cellular sterol content. ■

We thank Dr. Ulrike Beisiegel for supplying antibodies to apoE and for the FH fibroblasts and Dr. Jorgèn Gliemann for antibodies against LRP. We are grateful to David García, Susanna Castell, and Almudena García for their expert technical assistance and to Robin Rycroft for his expert editorial help. M. Fernández-Borja has a predoctoral fellowship from the Ministerio de Educación y Ciencia. E. Vilella has a postgraduate fellowship award from the Fundación Ferrer para la Investigación. This work was supported by the Comisión Interministerial de Ciencia y Tecnología (grant SAF 92-0897), the Fondo de Investigaciones Sanitarias from Ministerio de Sanidad (grant 93/0423E), and the European Community (BIOMED PL-921243).

Manuscript received 13 November 1995.

## REFERENCES

- Olivecrona, T., and G. Bengtsson-Olivecrona. 1989. Heparin and lipases. In Heparin. C. D. Lane and U. Lindahl, editors. Edward Arnold, London. 335–361.
- Eisenberg, S. 1990. Metabolism of apolipoproteins and lipoproteins. *Curr. Opin. Lipidol.* **1**: 205–215.
- Mahley, R. W., and M. M. Hussain. 1991. Chylomicron and chylomicron remnant catabolism. *Curr. Opin. Lipidol.* **2**: 170–176.
- Ginsberg, H. N. 1994. Lipoprotein metabolism and its relationship to atherosclerosis. *Lipid Disorders.* **78**: 1–20.
- Saxena, U., L. D. Witte, and I. J. Goldberg. 1989. Release of endothelial cell lipoprotein lipase by plasma lipoproteins and free fatty acids. *J. Biol. Chem.* **264**: 4349–4355.
- Hultin, M., G. Bengtsson-Olivecrona, and T. Olivecrona. 1992. Release of lipoprotein lipase to plasma by triacylglycerol emulsions. Comparison to the effect of heparin. *Biochim. Biophys. Acta.* **1125**: 97–103.
- Goldberg, I. J., J. J. Kandel, C. B. Blum, and H. N. Ginsberg. 1986. Association of plasma lipoproteins with postheparin lipase activities. *J. Clin. Invest.* **78**: 1523–1528.
- Vilella, E., J. Joven, M. Fernández, S. Vilaró, J. D. Brunzell, T. Olivecrona, and G. Bengtsson-Olivecrona. 1993. Lipoprotein lipase in human plasma is mainly inactive and associated with cholesterol-rich lipoproteins. *J. Lipid Res.* **34**: 1555–1564.
- Wallinder, L., J. Peterson, T. Olivecrona, and G. Bengtsson-Olivecrona. 1984. Hepatic and extrahepatic uptake of intravenously injected lipoprotein lipase. *Biochim. Biophys. Acta.* **795**: 513–524.
- Vilaró, S., M. Llobera, G. Bengtsson-Olivecrona, and T. Olivecrona. 1988. Lipoprotein lipase uptake from the liver: localization, turnover, and metabolic role. *Am. J. Physiol.* **254**: G711–G722.
- Beisiegel, U., W. Weber, and G. Bengtsson-Olivecrona. 1991. Lipoprotein lipase enhances the binding of chylomicrons to low density receptor-related protein. *Proc. Natl. Acad. Sci. USA.* **88**: 8342–8346.
- Beisiegel, U., A. Krapp, W. Weber, and G. Olivecrona. 1994. The role of  $\alpha_2$ M receptor/LRP in chylomicron remnant metabolism. *Ann. NY Acad. Sci.* **737**: 53–69.
- Felts, J. M., H. Itakura, and T. R. Crane. 1975. The mechanism of assimilation of constituents of chylomicrons, very low density lipoproteins and remnants. A new theory. *Biochem. Biophys. Res. Commun.* **66**: 1467–1475.
- Rumsey, S. C., J. C. Obunike, Y. Arad, R. J. Deckelbaum, and I. J. Goldberg. 1992. Lipoprotein lipase-mediated uptake and degradation of low density lipoproteins by fibroblasts and macrophages. *J. Clin. Invest.* **90**: 1504–1512.
- Williams, K. J., G. M. Fless, K. A. Petrie, M. L. Snyder, R. W. Brocia, and T. L. Swenson. 1992. Mechanisms by which lipoprotein lipase alters cellular metabolism of lipoprotein[a], low density lipoprotein, and nascent lipoproteins. *J. Biol. Chem.* **267**: 13284–13292.
- Eisenberg, S., E. Schayek, T. Olivecrona, and I. Vlodavsky. 1993. Lipoprotein lipase enhances binding of lipoproteins to heparan sulfate on cell surfaces and extracellular matrix. *J. Clin. Invest.* **90**: 2013–2021.
- Mulder, M., P. Lombardi, H. Jansen, T. J. C. van Berkel, R. R. Frants, and L. M. Havekes. 1992. Heparan sulphate proteoglycans are involved in the lipoprotein lipase-mediated enhancement of the cellular binding of very low



- density and low density lipoproteins. *Biochem. Biophys. Res. Commun.* **185**: 582-587.
18. Mulder, M., P. Lombardi, H. Jansen, T. J. C. Berkel, R. R. Frants, and L. M. Havekes. 1993. Low density lipoprotein receptor internalizes low density and very low density lipoprotein that are bound to heparan sulfate proteoglycans via lipoprotein lipase. *J. Biol. Chem.* **268**: 9369-9375.
  19. Chappel, D. A., G. L. Fry, M. A. Waknitz, L. E. Muhonen, M. W. Pladet, P-H. Iverius, and D. K. Strickland. 1993. Lipoprotein lipase induces catabolism of normal triglyceride-rich lipoproteins via the low density lipoprotein receptor-related protein/ $\alpha_2$ -macroglobulin receptor in vitro. *J. Biol. Chem.* **268**: 14168-14175.
  20. Nykjaer, A., G. Bengtsson-Olivecrona, A. Lookene, S. K. Moestrup, C. M. Petersen, W. Weber, U. Beisiegel, and J. Gliemann. 1993. The  $\alpha_2$ -macroglobulin receptor/low density lipoprotein receptor related protein binds lipoprotein lipase and  $\beta$ -migrating very low density lipoprotein associated with the lipase. *J. Biol. Chem.* **268**: 15048-15055.
  21. Obunike, J. C., I. J. Edwards, S. C. Rumsey, L. K. Curtiss, W. D. Wagner, R. J. Deckelbaum, and I. J. Goldberg. 1994. Cellular differences in lipoprotein lipase-mediated uptake of low density lipoproteins. *J. Biol. Chem.* **269**: 13129-13135.
  22. Sehayek, E., T. Olivecrona, G. Bengtsson-Olivecrona, I. Vlodasky, H. Levkovitz, R. Avner, and S. Eisenberg. 1995. Binding to heparan sulfate is a major event during catabolism of lipoprotein lipase by HepG2 and other cell cultures. *Arteriosclerosis*. **114**: 1-8.
  23. Herz, J. 1993. The LDL-receptor-related protein: portrait of a multifunctional receptor. *Curr. Opin. Lipidol.* **4**: 107-113.
  24. Lund, H., K. Takahashi, R. L. Hamilton, and R. J. Havel. 1989. Lipoprotein binding and endosomal itinerary of the low density lipoprotein receptor-related protein in rat liver. *Proc. Natl. Acad. Sci. USA.* **86**: 9318-9322.
  25. Beisiegel, U., W. Weber, G. Ihrke, J. Herz, and K. K. Stanley. 1989. The LDL-receptor-related protein, LRP, is an apolipoprotein E-binding protein. *Nature.* **341**: 162-164.
  26. Kowal, R. C., J. Herz, J. L. Goldstein, V. Esser, and M. S. Brown. 1989. Low density lipoprotein receptor-related protein mediates uptake of cholesteryl esters derived from apoprotein E-enriched lipoproteins. *Proc. Natl. Acad. Sci. USA.* **86**: 5810-5814.
  27. Hussain, M. M., F. R. Maxfield, J. Más-Oliva, I. Tabas, Z. Ji, T. L. Innerarity, and R. W. Mahley. 1991. Clearance of chylomicron remnants by the low density lipoprotein receptor-related protein/ $\alpha_2$ -macroglobulin receptor. *J. Biol. Chem.* **266**: 13936-13940.
  28. Willnow, T. E., Z. Sheng, S. Ishibashi, and J. Herz. 1994. Inhibition of hepatic chylomicron remnant uptake by gene transfer of a receptor antagonist. *Science.* **264**: 1471-1474.
  29. Herz, J., S. Q. Qui, A. Oesterle, H. V. DeSilva, S. Shafi, and R. J. Havel. 1995. Initial hepatic removal of chylomicron remnants is unaffected but endocytosis is delayed in mice lacking the low density lipoprotein receptor. *Proc. Natl. Acad. Sci. USA.* **92**: 4611-4615.
  30. Chappell, D. A., G. L. Fry, M. A. Waknitz, P-H. Iverius, S. E. Williams, and D. K. Strickland. 1992. The low density lipoprotein receptor-related protein/ $\alpha_2$ -macroglobulin receptor binds and mediates catabolism of bovine milk lipoprotein lipase. *J. Biol. Chem.* **267**: 25764-25767.
  31. Williams, S. E., I. Inoue, H. Tran, G. L. Fry, M. W. Pladet, P-H. Iverius, J-M. Lalouel, D. A. Chappell, and D. K. Strickland. 1994. The carboxyl-terminal domain of lipoprotein lipase binds to the low density lipoprotein receptor-related protein/ $\alpha_2$ -macroglobulin receptor (LRP) and mediates binding of normal very low density lipoproteins to LRP. *J. Biol. Chem.* **269**: 8653-8658.
  32. Nykjaer, A., M. Nielsen, A. Lookene, N. Meyer, H. Roigaard, M. Etzerod, U. Beisiegel, G. Olivecrona, and J. Gliemann. 1994. A carboxyl-terminal fragment of lipoprotein lipase binds to the low density lipoprotein receptor-related protein and inhibits lipase-mediated uptake of lipoprotein in cells. *J. Biol. Chem.* **269**: 31747-31755.
  33. Beisiegel, U. 1995. Receptors for triglyceride-rich lipoproteins and their role in lipoprotein metabolism. *Curr. Opin. Lipidol.* **6**: 117-122.
  34. Imber, M. J., and S. V. Pizzo. 1981. Clearance and binding of two electrophoretic "fast" forms of human  $\alpha_2$ -macroglobulin. *J. Biol. Chem.* **256**: 8134-8139.
  35. Bengtsson-Olivecrona, G., and T. Olivecrona. 1991. Phospholipase activity of milk lipoprotein lipase. *Methods Enzymol.* **197**: 345-356.
  36. Schumaker, V. N., and D. L. Puppione. 1986. Sequential flotation ultracentrifugation. *Methods Enzymol.* **128**: 155-170.
  37. Slot, J. W., H. J. Geuze, S. Gigengack, G. E. Lienhard, and D. E. James. 1991. Immunolocalization of the insulin regulatable glucose transporter in brown adipose tissue of the rat. *J. Cell Biol.* **113**: 123-135.
  38. Kristensen, T., S. K. Moestrup, J. Gliemann, L. Bendtsen, O. Sand, and L. Sottrup-Jensen. 1990. Evidence that newly cloned low-density-lipoprotein receptor related protein (LRP) is the  $\alpha_2$ -macroglobulin receptor. *FEBS Lett.* **276**: 151-155.
  39. Fernández-Borja, M., D. Bellido, R. Makiya, G. David, G. Olivecrona, M. Reina, and S. Vilaró. 1994. The actin cytoskeleton of fibroblasts organizes surface proteoglycans that bind basic fibroblast growth factor and lipoprotein lipase. *Cell Motil. Cytoskel.* **30**: 98-107.
  40. Posner, B. I., B. A. Patel, M. N. Khan, and J. J. M. Bergeron. 1982. Effect of chloroquine on internalization of  $^{125}$ I-insulin into subcellular fractions of rat liver. Evidence for an effect of chloroquine on Golgi elements. *J. Biol. Chem.* **257**: 5789-5799.
  41. Rapraeger, A. C. 1993. The coordinated regulation of heparan sulfate, syndecans and cell behaviour. *Curr. Opin. Cell Biol.* **5**: 844-853.
  42. Goldstein, J. L., S. K. Basu, and M. S. Brown. 1983. Receptor-mediated endocytosis of low-density lipoprotein in cultures cells. *Methods Enzymol.* **98**: 241-260.
  43. Herz, J., R. C. Kowal, Y. K. Ho, M. S. Brown, and J. L. Goldstein. 1990. Low density lipoprotein receptor-related protein mediates endocytosis of monoclonal antibodies in cultured cells and rabbit liver. *J. Biol. Chem.* **265**: 21355-21362.
  44. Yanagishita, M. 1992. Glycosylphosphatidylinositol-anchored and core protein-intercalated heparan sulfate proteoglycans in rat ovarian granulosa cells have distinct secretory, endocytic, and intracellular degradative pathways. *J. Biol. Chem.* **267**: 9505-9511.
  45. Sivaram, P., S. Y. Choi, L. K. Curtiss, and I. J. Goldberg. 1994. An amino-terminal fragment of apolipoprotein B binds to lipoprotein lipase and may facilitate its binding to endothelial cells. *J. Biol. Chem.* **269**: 9409-9412.
  46. Goldstein, J. L., and M. S. Brown. 1974. Binding and degradation of low density lipoproteins by cultured hu-

- man fibroblasts. Comparison of cells from a normal subject and from a patient with homozygous familial hypercholesterolemia. *J. Biol. Chem.* **249**: 5153–5162.
47. Attie, A. D., R. C. Pittman, Y. Watanabe, and D. Steinberg. 1981. Low density lipoprotein receptor deficiency in cultured hepatocytes of the WHHL rabbit. Further evidence of two pathways for catabolism of exogenous proteins. *J. Biol. Chem.* **256**: 9789–9792.
48. Camejo, G., G. Fager, B. Rosengren, E. Hurt-Camejo, and G. Bondjers. 1993. Binding of low density lipoproteins by proteoglycans synthesized by proliferating and quiescent human arterial smooth muscle cells. *J. Biol. Chem.* **268**: 14131–14137.
49. Edwards, I. J., I. J. Goldberg, J. S. Parks, H. Xu, and W. D. Wagner. 1993. Lipoprotein lipase enhances the interaction of low density lipoproteins with artery-derived extracellular matrix proteoglycans. *J. Lipid Res.* **34**: 1155–1163.
50. Beisiegel, U., W. J. Schneider, J. L. Goldstein, R. G. W. Anderson, and M. S. Brown. 1981. Monoclonal antibodies to the low density lipoprotein receptor as probes for study of receptor-mediated endocytosis and the genetics of familial hypercholesterolemia. *J. Biol. Chem.* **256**: 11923–11931.
51. Gannoun-Zaki, L., I. Pieri, J. Badet, M. Moenner, and D. Barritault. 1991. Internalization of basic fibroblast growth factor by Chinese hamster lung fibroblast cells: involvement of several pathways. *Exp. Cell Res.* **197**: 272–279.
52. Roghani, M., and D. Moscatelli. 1992. Basic fibroblast growth factor in internalized through both receptor-mediated and heparan sulfate-mediated mechanisms. *J. Biol. Chem.* **267**: 22156–22162.
53. Reiland, J., and A. C. Rapraeger. 1993. Heparan sulfate proteoglycan and FGF receptor target basic FGF to different intracellular destinations. *J. Cell Sci.* **105**: 1085–1093.
54. Tabas, I., S. Lim, X-X. Xu, and F. R. Maxfield. 1990. Endocytosed  $\beta$ -VLDL and LDL are delivered to different intracellular vesicles in mouse peritoneal macrophages. *J. Cell Biol.* **111**: 929–940.
55. Lombardi, P., M. Mulder, H. van der Boom, R. R. Frants, and L. M. Havekes. 1993. Inefficient degradation of triglyceride-rich lipoprotein by HepG2 cells is due to a retarded transport to the lysosomal compartment. *J. Biol. Chem.* **268**: 26113–26119.
56. Williams, K. J., K. A. Petrie, R. W. Brocia, and T. L. Swenson. 1991. Lipoprotein lipase modulates net secretory output of apolipoprotein B in vitro: a possible pathophysiologic explanation for familial combined hyperlipidemia. *J. Clin. Invest.* **88**: 1300–1306.
57. Olivecrona, T., and G. Bengtsson-Olivecrona. 1993. Lipoprotein lipase and hepatic lipase. *Curr. Opin. Lipidol.* **4**: 187–196.
58. Shepherd, J., and C. J. Packard. 1986. Receptor-independent low-density lipoprotein metabolism. *Methods Enzymol.* **129**: 566–590.
59. Chajek-Shaul, T., G. Friedman, G. Bengtsson-Olivecrona, I. Vlodavsky, and R. Bar-Shavit. 1990. Interaction of lipoprotein lipase with subendothelial extracellular matrix. *Biochim. Biophys. Acta.* **1042**: 168–175.
60. Saxena, U., E. Ferguson, and C. L. Bisgaier. 1993. Apolipoprotein E modulates low density lipoprotein retention by lipoprotein lipase anchored to subendothelial matrix. *J. Biol. Chem.* **268**: 14812–14819.